Journal of Immunotoxicology

http://informahealthcare.com/imt
ISSN: 1547-691X (print), 1547-6901 (electronic)
J Immunotoxicol, Early Online: 1–8

DOI: 10.3109/1547691X.2013.851747

informa
healthcare

RESEARCH ARTICLE

Effects of short-term oral combined exposure to environmental immunotoxic chemicals in mice

Risako Nishino, Tomoki Fukuyama, Tadashi Kosaka, Koichi Hayashi, Yuko Watanabe, Yoshimi Kurosawa, Hideo Ueda, and Takanori Harada

The Institute of Environmental Toxicology, Ibaraki, Japan

Abstract

People are constantly exposed to environmental chemicals through contact with the atmosphere or by ingestion of food. Therefore, when conducting safety assessments, the immunotoxic effects of combinations of chemicals in addition to toxicities produced by each chemical alone should be considered. The objective of the studies reported here were to demonstrate the combined effects of three well-known environmental immunotoxic chemicals – methoxychlor (MXC), an organochlorine compound; parathion (PARA), an organophosphate compound; and piperonyl butoxide (PBO), an agricultural insecticide synergist – by using a short-term oral exposure method. Seven-week-old Balb/cAnN mice received daily oral exposure to either one or two of the environmental immunotoxic chemicals for 5 consecutive days. On Day 2, all mice in each group were immunized with sheep red blood cells (SRBC), and their SRBC-specific IgM responses were analyzed by using an enzyme-linked immunosorbent assay and plaque-forming cell assay. T- and B-cell counts in the mouse spleens were also assessed via surface antigen expression. Mice that received MXC + PARA and PBO + MXC treatment showed marked decreases in SRBC-specific IgM production and T- and B-cell counts compared with those in mice that received vehicle control or the corresponding individual test substance. This suggests that simultaneous exposure to multiple environmental chemicals increases the immunotoxic effects of the chemicals compared to individual exposure.

Keywords

Acquired immunotoxicity, combined toxicity, methoxychlor, parathion, piperonyl butoxide

History

Received 30 July 2013
Revised 10 September 2013
Accepted 1 October 2013
Published online 4 November 2013

Introduction

Humans are exposed daily to a vast range of products that contain environmental agents (e.g. cosmetics, pesticides, drugs, and biotechnology-derived products) and to multiple environmental chemicals in the atmosphere and in food (Gilbert et al., 2011; Groten et al., 1997; Kortenkamp et al., 2007; Teuschler et al., 2002). Because of this constant exposure, when conducting safety assessments one must take into consideration the effects of combined exposure. For example, combined exposure to pesticides and heavy metals is known to enhance overall toxicity compared with that from exposure to the individual agents (Institoris et al., 1999, 2002). Approaches to assess effects from combined exposures have been described (Feron et al., 1995; Groten et al., 2001; Hernandez et al., 2013; Simmons, 1995). However, most toxicity assessments are conducted based on exposure to individual substances and, as such, mechanisms of effects from combined exposure to environmental chemicals remain unclear. Therefore, the objective of the studies reported here were to investigate the combined toxicologic effects of multiple chemicals.

In the study reported here, the toxic effects from combined exposure to three common environmental chemicals were investigated by examining the impact on immune functions. It is well known that exposure to environmental agents can compromise immunologic function (Fukuyama et al., 2010, 2013; Nishino et al., 2013). For example, several animal studies have shown there are alterations of primary humoral responses induced by immunotoxicants like dioxins and pesticides (Flipo et al., 1992; Smialowicz et al., 1997). To avoid these risks, immunotoxicity tests have been developed for evaluating the safety of environmental chemicals and pharmaceuticals (Holsapple, 2003; Luster et al., 1988). Based on those analyses, guidelines have been introduced over the years to regulate exposure to many agents; these include those published by the US Environmental Protection Agency (EPA, 1998), the Food and Drug Administration (FDA, 2002), the European Medicines Agency (Committee for Proprietary Medicinal Products, 2000), and the International Conference on Harmonization (ICH, 2006).

Our laboratories previously developed a short-term oral exposure method for assessment of the immunosuppressive potential of environmental chemicals (Fukuyama et al., 2013). In the current study, using this method, we demonstrate the combined immunotoxic effects of three well-known environmental chemicals, i.e. methoxychlor (MXC) – an organochlorine compound, parathion (PARA) – an organophosphate compound, and piperonyl butoxide (PBO) – an agricultural insecticide synergist. These three chemicals were selected on the basis of previous studies: MXC exposure causes atrophy of $CD4^+CD8^+$ T-cells in the thymus (Takeuchi et al., 2002a,b); PARA markedly inhibits antigen-specific IgM production (Casale et al., 1984); and PBO depletes T-cells in the spleen and thymus, induces bone

Address for correspondence: Dr Tomoki Fukuyama, Laboratory of Immunotoxicology and Acute Toxicology, Toxicology Division, Institute of Environmental Toxicology, Uchimoriya-machi 4321, Joso-shi, Ibaraki 303-0043, Japan. Tel: 81297274628. Fax: 81297274518. E-mail: fukuyama@iet.or.jp

marrow hypoplasia, and inhibits T-cell proliferation in lymphoid tissues (Diel et al., 1999; Battaglia et al., 2010; Mitsumori et al., 1996). We also previously showed that MXC, PARA, and PBO exposure results in increased thymocyte apoptosis, markedly inhibited sheep red blood cell (SRBC)-specific IgM production, and aggravation of immune disorders such as atopic dermatitis and allergic airway inflammation (Fukuyama et al., 2011; Nishino et al., 2013).

Materials and methods

Chemicals

Standard MXC ($C_{16}H_{15}Cl_3O_2$, >97% pure), standard PARA ($C_{10}H_{14}NO_5PS$, 99.5% pure), standard PBO ($C_{19}H_{30}O_5$, >98% pure), and dimethyl sulfoxide (DMSO) were purchased from Wako Pure Chemical Industries, Ltd. (Osaka, Japan). Corn oil was purchased from Hayashi Chemicals (Tokyo, Japan). For the *in vivo* portion of this study, MXC, PARA, or PBO diluted in corn oil to a fixed final volume was orally administered to mice. Based on the EPA Immunotoxicity Guidelines (1998) that states doses should 'not produce significant stress, malnutrition, or fatalities', doses used in this study were < 1/5 the median lethal dose (LD_{50}; dose at which ≥50% of animals would be expected to die) and administered concurrently to avoid induction of clear general or immune toxicity (i.e. changes in appearance, posture, behavior, respiration, consciousness, neurologic status, temperature, excretion, etc.) (Fukuyama et al., 2013). The single-chemical dosages used in this study were: MXC, 100 mg/kg day; PARA, 1.0 mg/kg day; and PBO, 100 mg/kg day. Combination dosages were prepared by mixing each chemical so that the final concentration of each chemical was half that of the single dosage. Actually, there were no abnormal signs during the examination period. With regard to body weight measurements, treated groups' values were comparable with those of the vehicle control and intact groups (data not shown). Therefore, we selected relatively high doses compared with actual human exposures. Actual doses and preparation of the test substances are presented in Table 1.

Animals

Balb/cAnN mice (female, 6-weeks-old) were purchased from Charles River Laboratories (Atsugi, Kanagawa, Japan) and housed individually in cages under controlled lighting (lights on, 07:00–19:00), temperature (22 ± 3 °C), humidity (55% ± 15%), and ventilation (at least 10 complete fresh-air changes/h). Standard rodent chow (Certified Pellet Diet MF; Oriental Yeast Co., Tokyo) and filtered water were available *ad libitum*.

Female mice were selected as the model for this study because the EPA Immunotoxicity Guidelines (EPA, 1998) consider the mouse a model species for use in immunotoxicity studies that examine effects of agricultural chemicals (see Casale et al., 1984; Diel et al., 1999; Battaglia et al., 2010). The guideline indicates that either rats or mice may be used. Additionally, if ADME data are similar between species, then either rats or mice may be used. According to our preliminary immunotoxicity study data for MXC, PARA, and PBO, mice were more sensitive than rats. Therefore, we selected mice for the current study. Furthermore, in immunotoxicity studies, only one gender need be evaluated; in general, females are considered to yield more consistent outcomes than male animals when evaluating humoral immune responses. Consequently, Balb/cAnN mice were selected because our laboratory has historical immunotoxicity study data for our selected chemicals on this strain (data not shown). All aspects of the current study were conducted in accordance with the Animal Care and Use Program of the Institute of Environmental Toxicology, Japan (IET IACUC Approval No. 12027).

Chemical exposure of mice

After a 1-week acclimatization period, mice (now 7-weeks-old) were allocated randomly to two groups ($n = 8$ mice/group): treatment/vehicle control and to a no treatment (intact group). On Days 1–5, mice were given an oral dose (by gavage, without anaesthesia) of a single or combination test solution (MXC, PARA, PBO, MXC + PARA, PARA + PBO, PBO + MXC) or vehicle only. On Day 2, a solution of SRBC (6×10^7 cells/animal; Nippon Bio-Supp. Center, Tokyo) was injected via the tail vein into all test and control mice for immunization. One day after the final oral administration (i.e. on Day 6 of study), all mice were anaesthetized with Isoflurane and blood samples taken from the inferior vena cava. Serum samples were assayed for SRBC-specific serum IgM. After exsanguination from the abdominal aorta, the thymus of each animal was carefully removed and weighed. The spleen was removed and placed in phosphate-buffered saline (PBS, pH 7.4; Life Technologies Co., Ltd., Tokyo). Single-cell splenocyte suspensions in 5 ml modified Eagle's medium supplemented with 5% heat-inactivated fetal bovine serum (FBS, Life Technologies) were prepared by passage through a stainless-steel screen and sterile 70-μm nylon cell strainer (Falcon, Tokyo). Numbers of lymphocytes in each suspension were determined using a Z2 Coulter Counter (Beckman Coulter, Tokyo).

Determination of serum SRBC-specific IgM response

Levels of SRBC-specific IgM in the serum were determined using a modified version of the method of Temple et al. (1993). In brief, SRBC-membrane antigen was extracted with Tris-HCl and 0.1% sodium dodecyl sulfate in PBS. The samples were then dialyzed for 2 days against PBS. The protein content of each conjugated sample was determined using the method of Lowry et al. (1951). SRBC-specific IgM levels were then measured by means of enzyme-linked immunosorbent assay (ELISA) in flat-bottomed microplates (Nalge Nunc, Tokyo) whose wells had been coated with SRBC-membrane antigen (2 μg/ml coating buffer; BD Pharmingen, Tokyo) during an overnight incubation at 4 °C. Following washing of each well 5-times with wash buffer (BD Pharmingen) and blocking of potential non-specific binding by incubation for 2 h at room temperature (RT) with assay diluent (BD Pharmingen), a dilution of each mouse serum sample (in assay diluent, from 1:4 to 1:16384) was added to each well and the plates incubated a further 2 h at RT. After gentle rinsing with wash buffer to remove all unbound materials, peroxidase-conjugated anti- mouse IgM (secondary antibody, Rockland Inc., Gilbertsville, PA; dilution 1:15 000) was added to each well and

Table 1. Chemicals and dose settings.

Test substance	Type	LD_{50} (mg/kg)	Dose (mg/kg day)
Methoxychlor ($C_{16}H_{15}C_{13}O_2$)	Organochlorine compound	2900	100
Parathion ($C_{10}H_4NO_5PS$)	Organophosphate pesticide	5	1
Piperonyl butoxide ($C_{19}H_{30}O_5$)	Insecticide synergist	2600	100

the plate incubated for 2 h at RT. The wells were then rinsed again to remove non-adherent anti-mouse IgM. Finally, to quantify the amount of bound antibodies in each well, tetramethylbenzidine (100 µl/well) was added to each well and the plate incubated in the dark at RT for 30 min. Optical density was then measured at 450 nm by in a Spectra MAX 190 microplate reader (Molecular Devices, Osaka).

Assessment of the splenocyte IgM plaque-forming cell response to SRBC

The IgM plaque-forming cell (PFC) response to SRBC was determined using a modified version of the methods of Cunningham (1965) and Jerne & Nordin (1963). Briefly, $\approx 1 \times 10^6$ cells were incubated with 1% SRBC and a 1:30 dilution of guinea pig complement (Denka Seiken Co., Tokyo) for 10 min at 4 °C. The cells were then applied to a Cunningham chamber (Takahashi Giken Glass Co., Tokyo) and incubated for 1.5 h at 37 °C in a 5% CO_2 atmosphere. The number of plaques in each sample was then counted using a stereomicroscope.

Flow cytometric analysis

Isolated splenocytes were stained all at one time with fluorescein isothiocyanate (FITC)- conjugated anti-peanut agglutinin (Vector Laboratories, Inc., Burlingame, CA) and the monoclonal antibodies (MAb) phycoerythrin-cyanine-7-conjugated anti-mouse CD4 (PE-Cy7, clone RM- 4-5), allophycocyanin-cyanine-7-conjugated anti-mouse CD8 (APC-Cy7, clone 53-6.7), APC-conjugated anti-mouse CD3 (clone 145-2C11), and peridinin chlorophyll protein-Cy5.5-conjugated rat anti-mouse CD19 (PerCP-Cy5, clone 1D3 (all BD Pharmingen). To avoid non-specific binding, 10^6 cells were incubated with 1 µg Mouse F_c BlockTM (BD Pharmingen) for 5 min at RT, followed by incubation with MAb for 30 min at 4 °C in the dark. Cells were then washed twice with 5% FBS in PBS, re-suspended at 10^6 cells/tube in 500 µl PBS and then analyzed on a FACSVerse flow cytometer (BD Pharmingen) using FACSuite software. A minimum of 20 000 events/sample was collected and analyzed for antigen expression.

Statistical analysis

All data are expressed as mean ± standard deviation (SD). Analysis of variance (ANOVA) was used to evaluate the results. For significant results, differences between vehicle control and treatment groups were then assessed using a Dunnett's multiple comparison test. Statistical significance of differences between single-chemical and combination-treatment groups was determined using a Student's *t*-test. p values <0.05 were considered significant in each test.

Results

Overall toxicity of the various treatments to the mice

Throughout the studies, there were no abnormal clinical signs (e.g. decreased activity) or changes in body weight or body weight gain due to any of the treatment regimens.

Thymus weights

Thymus weights are shown in Figure 1. All treatment groups had significantly ($p<0.01$) decreased values compared with those seen with the vehicle control mice. The MXC + PARA mice did display a significant decrease (≈22.2%, $p<0.01$) compared against the values for the PARA treatment mice, and also a decrease of 8.1% versus MXC mice; however, this decrease was not significant. The PBO + MXC mice had average decreases of thymus weight of ≈13.0% vs the PBO hosts, but this decrease too was not significant. Thymus weights in the PARA + PBO mice were comparable with those of the PARA or PBO hosts.

Serum SRBC-specific IgM responses

Serum SRBC-specific IgM responses are shown in Figure 2. In the PARA, PBO, and PARA + PBO treatment groups, SRBC-specific IgM responses were comparable with that of the vehicle control group. However, the MXC + PARA and PBO + MXC treatment groups displayed significantly decreased ($p<0.05$) SRBC-specific IgM responses compared with that by the vehicle controls – decreases of ≈40.9% and 29.5%, respectively. Furthermore, the MXC + PARA- treated mice had a significantly decreased (≈41.8%) response compared with that of the MXC-only mice. Further, while the MXC + PARA mice displayed a decreasing trend in response compared with that by the PARA-only mice, the net difference (a decrease of ≈36.3%) was not significant. Similarly, the PBO + MXC mice had a significantly decreased response compared with the PBO ≈29.2%, $p<0.05$) and MXC (30.6%, $p<0.01$) treatment mice.

Splenocyte IgM PFC response to SRBC

Splenocyte IgM PFC responses to SRBC are shown in Figure 2. All treatment groups had significantly ($p<0.01$) lower IgM PFC responses to SRBC compared with the vehicle control mice. The MXC + PARA mice had decreases of ≈22.7% vs the MXC and 29.9% vs the PARA groups, but the decreases were not significant. However, PBO + MXC treatment did cause a significant decrease (≈38.3%, $p<0.01$) from PBO mice values; there

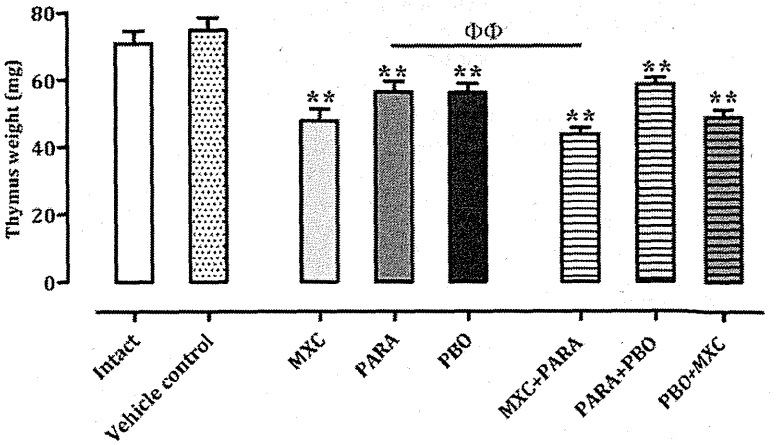

Figure 1. Absolute thymus weights. Mice were treated with nothing (intact naive), vehicle, methoxychlor (MXC), parathion (PARA), piperonyl butoxide (PBO), or combinations of the agents (two at a time). Absolute thymus weights are expressed as mean ± SD (mg; $n=8$ per group). **$p<0.01$ (Dunnett's multiple comparison test) vs vehicle control group; ΦΦ $p<0.01$ (Student's *t*-test) vs single test substance groups.

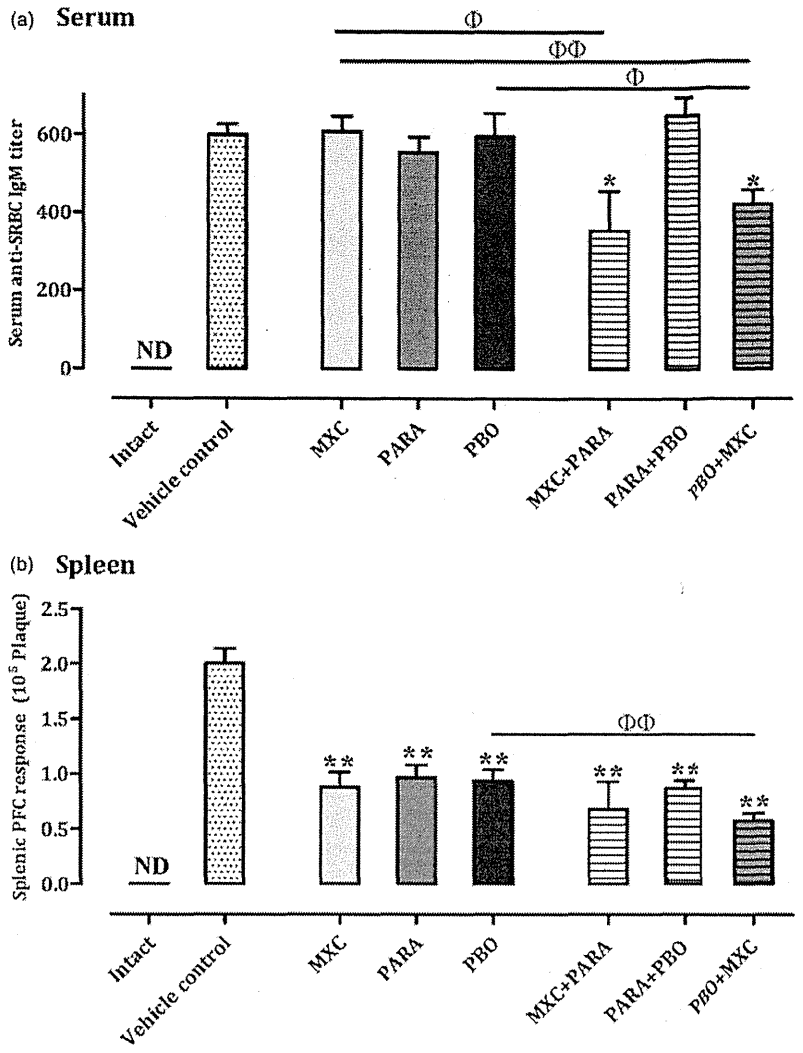

Figure 2. Serum and splenic IgM responses. Mice were treated as described in the Figure 1 legend. (a) Serum and (b) spleen IgM responses are shown. IgM responses are expressed as mean ± SD (titre; $n = 8$ per group). IgM responses in the spleen are expressed as mean ± SD ($n = 8$ per group). $^*p < 0.05$ and $^{**}p < 0.01$ (Dunnett's multiple comparison test) vs vehicle control group; $\Phi p < 0.05$ and $\Phi\Phi p < 0.01$ (Student's *t*-test) vs single test substance groups.

was a decrease of ≈34.1% vs MXC mice values, but this was not significant. Splenocyte PFC responses with PARA + PBO mice were comparable to that seen with their PARA- or PBO-only counterparts.

Splenocyte T-cell counts

To evaluate the level of T-cell immunosuppression following the single or combination treatments, isolated lymphocytes were stained with anti-CD3, -CD4, and -CD8 antibodies. The numbers of total, helper, and cytotoxic T-cells are shown in Figure 3. In the MXC, PARA, PBO, PARA + PBO, and PBO + MXC treatment groups, all T-cell counts were comparable with those of the vehicle control group. The PBO + MXC group showed a decrease in T-cell counts, but this was not statistically significant. The MXC + PARA group had significantly decreased total ($p < 0.01$), helper ($p < 0.05$), and cytotoxic ($p < 0.01$) T-cell counts compared with those of control, MXC, and PARA mice – decreases of, respectively, ≈52.5, 42.8, and 58.0% vs control; 42.1, 26.1, and 49.9% vs MXC alone; and 33.2, 20.0, and 39.6% vs PARA alone.

Splenocyte B-cell counts

To evaluate B-cell immunosuppression following the single or combination treatments, isolated lymphocytes were stained with anti-CD19 and anti-peanut agglutinin (PNA) antibodies (Figure 4). In the MXC, PARA, PBO, PARA + PBO, and PBO + MXC treatment groups, total B-cell ($CD19^+$) counts were comparable with that in the vehicle controls. The PBO + MXC group had a decrease in total B-cell counts, but this was not significant. The MXC + PARA group had significantly decreased total B-cell counts ($p < 0.01$) compared with the vehicle control, MXC, and PARA groups – decreases of, respectively, ≈50.9, 36.1, and 33.8%.

In all of the groups given a test substance, germinal center B-cell ($CD19^+PNA^+$) counts were lower than that in the vehicle control mice. In addition, the MXC ($p < 0.05$) PBO ($p < 0.05$), MXC + PARA ($p < 0.05$), and PBO + MXC ($p < 0.01$) groups had significantly decreased germinal center B-cell counts compared with that of the vehicle controls. The PBO + MXC treatment mice also had significantly decreased ($p < 0.05$) germinal center B-cell counts compared with the PBO and MXC treatment group – decreases of ≈42.7 and 49.2%, respectively.

Discussion

Our objective was to provide new insights into effects of combined exposures to three well-known environmental chemicals: methoxychlor, parathion, and piperonyl butoxide. This study examined immunotoxic effects of these chemicals in Balb/cAnN mice using a short-term oral exposure protocol. Changes in host immune status were assessed by measures of effects on thymus

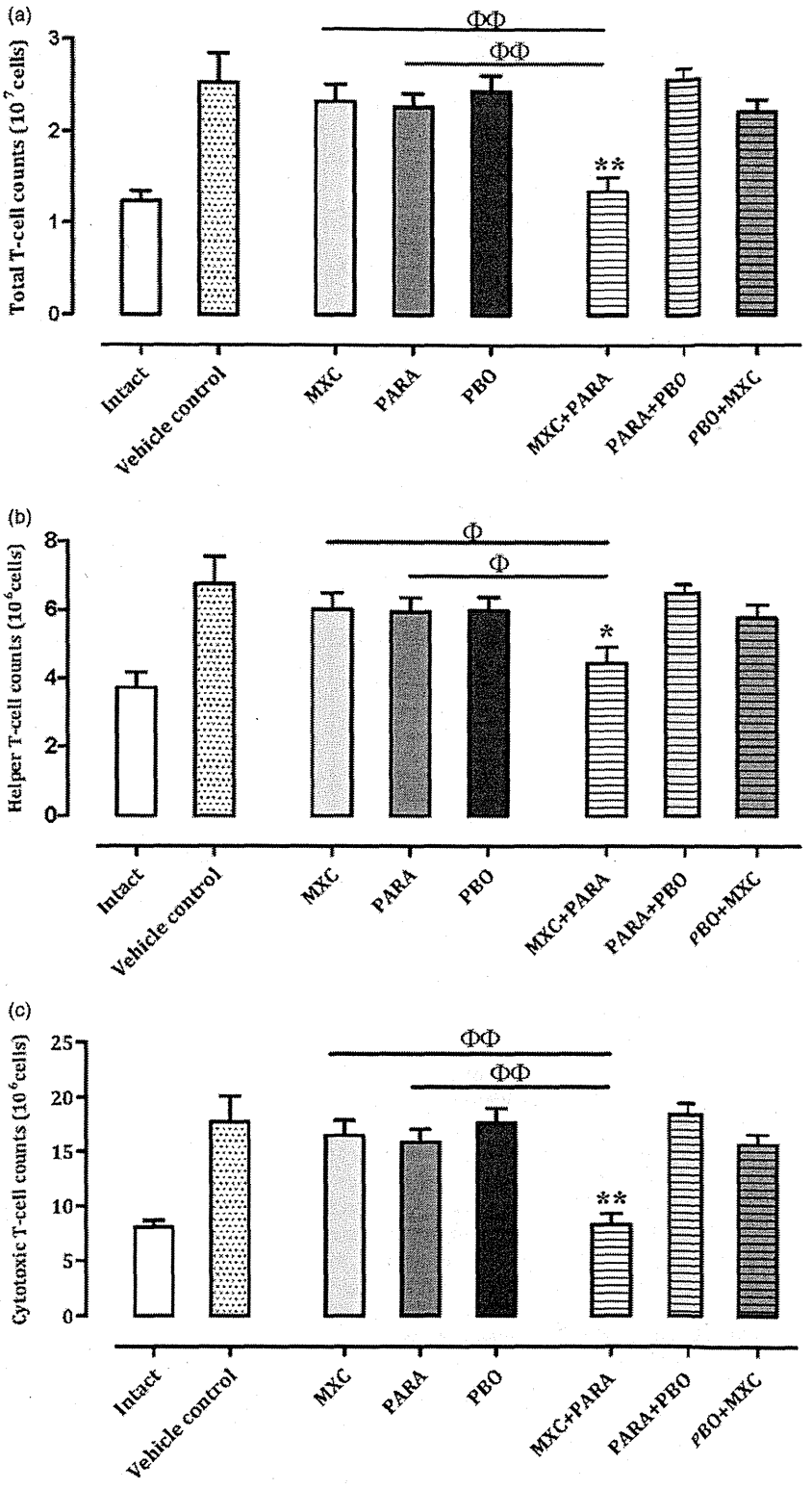

Figure 3. T-cell sub-type counts in spleens. Mice were treated as described in the Figure 1 legend. (a) Total, (b) helper, and (c) cytotoxic T-cell counts are shown. Results for intact, vehicle, and individual agent-treated mice are included in each chart. Cell counts are expressed as mean ± SD ($n = 8$ per group). $*p < 0.05$ and $**p < 0.01$ (Dunnett's multiple comparison test) vs vehicle control group; $\Phi p < 0.05$ and $\Phi\Phi p < 0.01$ (Student's t-test) vs single test substance groups.

weight, anti-SRBC IgM responses, and T- and B-cell counts in serum and spleen.

Based on our previous report (Fukuyama et al., 2010), immunosuppressive environmental chemicals induce thymocyte apoptosis and reduced thymus weights. Thus, changes in thymus weights were analyzed as a general measure of *in situ* immunotoxicity from the test agents here as the thymus is a key lymphoid organ, and precursor T-cells migrate there to undergo maturation (Janeway et al., 2004). In our study, compared to what was seen with vehicle control mice, all treatments induced significant decreases in thymus weight. Among the combined exposure groups, the MXC + PARA mice had values significantly decreased compared with those of PARA-only mice (but not vs MXC mice). In contrast, while PBO + MXC mice had a trend toward decreasing values vs the same PBO hosts, the decrease was not significant. PARA + PBO mice had values not altered

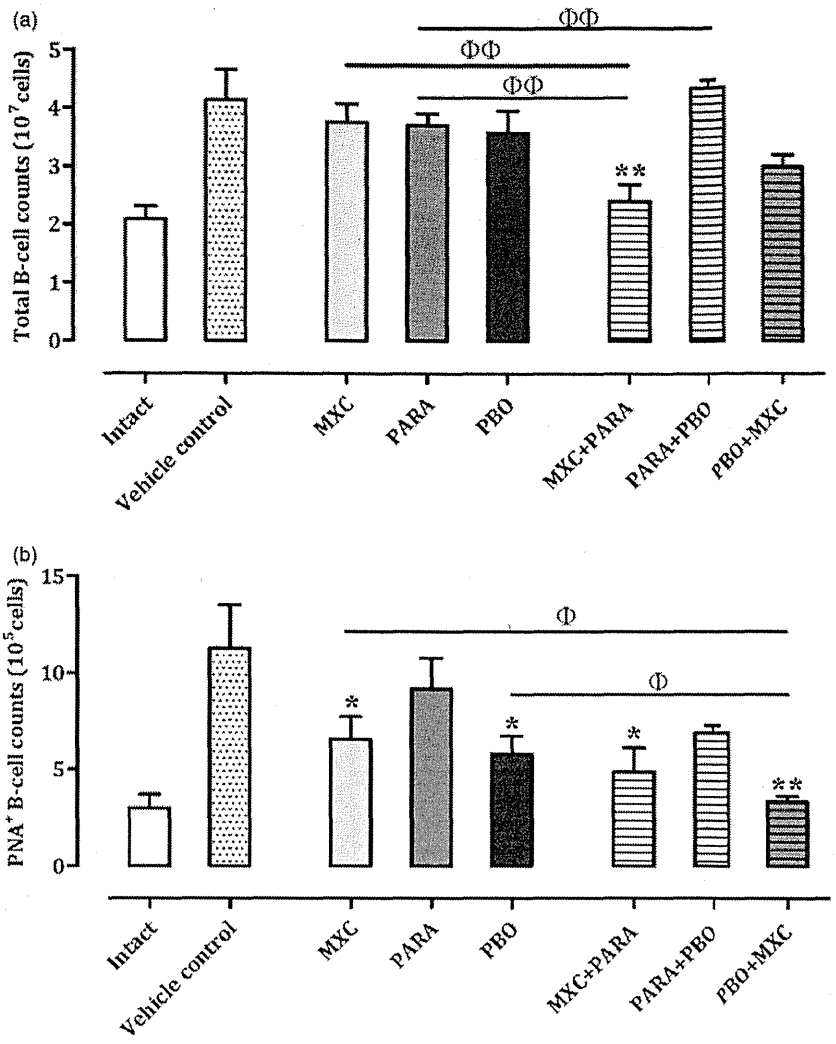

Figure 4. Total B-cell and germinal center B-cell counts in spleens. Mice were treated as described in the Figure 1 legend. (a) Total B-cell and (b) germinal center B-cell counts are shown. Results for intact, vehicle, and individual agent-treated mice are included in each chart. Cell counts are expressed as mean ± SD ($n = 8$ per group). *$p < 0.05$ and **$p < 0.01$ (Dunnett's multiple comparison test) vs vehicle control group; Φ$p < 0.05$ and ΦΦ$p < 0.01$ (Student's t-test) vs single test substance groups.

from their individual agent counterparts. These results suggested to us that, at the level of thymocyte damage (i.e. potential apoptosis), there was little to no interactive effect from the combined exposures to PARA + PBO and PBO + MXC exposures. In contrast, as MXC + PARA exposure appeared to have induced a more severe effect compared with exposure to each individual chemical, it is likely that some interactive effect (most likely synergistic) was occurring *in situ* to amplify the toxicities of each individual test agent. As will become clear below, this *preferentially* strong toxicity by MXC + PARA compared to the other combinational regimens becomes evident in several other aspects of these studies.

SRBC is a common antigen used to evaluate general immune status. After immunization with SRBC, SRBC-specific IgM responses in serum and spleen can be assessed using ELISA and PFC assays, respectively (Temple et al., 1993; White et al., 2010). Use of these two assays allows for evaluation of the mechanisms of action of xenobiotic-induced immunotoxicities (Herzyk & Holsapple, 2007). Compared with the vehicle control mice, MXC + PARA and PBO + MXC mice had significant decreases in serum SRBC-specific IgM responses, whereas MXC, PARA, PBO, and PARA + PBO mice did not. In addition, the IgM responses with the MXC + PARA mice were significantly decreased vs that of MXC mice, and PBO + MXC treatment led to significant decreases relative to those seen with PBO and MXC mice. In contrast, in all groups given a test substance, spleen SRBC-specific IgM PFC responses were significantly decreased relative to those seen with the vehicle control group. In addition, the SRBC-specific IgM responses with spleens from the PBO + MXC mice were significantly decreased compared to that of organs from PBO mice. Based on our historic data (Fukuyama et al., 2013), the peak response to SRBC for the SRBC-specific IgM ELISA occurs ~2 days after the maxima that would be used to optimize results for a PFC. Thus, as we utilized a protocol that was focusing mainly on the PFC assay, it is not a complete surprise that the SRBC-specific IgM ELISA responses were weaker than the PFC ones. Under these conditions, MXC + PARA and PBO + MXC led to significant decreases relative to those seen with PBO and MXC in serum SRBC-specific IgM responses. These results suggested to us that MXC + PARA or PBO + MXC exposures induced a more severe reduction in humoral immune responses compared with exposure to any of the three individual chemicals.

To further clarify mechanisms of MXC + PARA- or PBO + MXC-induced immunosuppression, total, helper, and cytotoxic T-cell counts, as well as total and germinal center B-cell counts in the spleens were analyzed via flow cytometry based on cell-specific surface makers (Janeway et al., 2004). It was clear that the MXC + PARA combined treatment damaged T-cells. Total, helper, and cytotoxic T-cell counts in hosts that received this combined treatment were decreased compared with those in vehicle control, MXC, and PARA mice. In contrast,

in the PBO + MXC hosts, the counts were comparable to those in PBO- and MXC-only mice. Similarly, in PARA + PBO mice, all sets of counts were comparable to those in PARA and PBO mice. These latter sets of results indicated that the toxicities of these two chemical combinations, at least in regard to impacts on T-cell populations *in situ*, were similar to those of any of their single chemical constituents. It is interesting to note that, with the MXC + PARA regimen, the changes in cell counts corresponded with the observed changes in SRBC-specific IgM responses. On the other hand, in the PBO + MXC group, although SRBC-specific IgM responses were decreased compared to the control, PBO, and MXC mice, there were no similar correspondence with the T-cell measures. This might suggest that the combined action of the PBO and MXC may have been directed more against the B-cell aspects of humoral responses than against T-cells; however, this still remains to be verified in more detailed studies.

In an immune response, local activated B-cells act as antigen-presenting cells for helper or cytotoxic T-cells (Goutet et al., 2005), proliferate, and differentiate into plasma cells to secrete antigen-specific antibodies. Some B-cells are activated at the T/B-cell border and migrate to form germinal centers (in primary follicles; Janeway et al., 2004); therefore, changes in the numbers of germinal centers and associated B-cells can reflect major responses to exposure to antigens or toxicants (Vieira & Rajewsky, 1990; Takahashi et al., 1998). A marked decrease in total B-cell counts was seen in the MXC + PARA-treated mice compared with that in MXC and PARA mice. Neither other combinational treatment had a similar significant effect. At the germinal center level, both MXC + PARA and PBO + MXC led to significant reductions in B-cell levels; PARA + PBO had no significant impact. Compared to their individual agents, MXC + PARA treatment caused even greater reductions in total B-cell levels, but had no effect at the germinal center level. This contrasts with PBO + MXC that had the opposite effect, i.e. no impact at total B-cell level but significantly-so at germinal centers. While these opposing outcomes are without explanation at this point, the upshot is that the combinational treatments with PBO + MXC or MXC + PARA are toxic to B-cells *in situ*. Toxicity from PARA + PBO is nominal at best.

The findings with the PBO + MXC mice supports our contention cited in the early paragraphs about potentially more selective effects on B-cells. That the MXC + PARA regimen also impacted on B-cells (beyond above-noted effects on thymic weights, T-cell counts, and IgM responses) suggested that this specific combination displayed a far more immunotoxic targeting than the other combined regimen. Whether such a divergent effect is due to differences in synergizing effects from each individual agent is an interesting possibility. Future studies with gradational combinations of each test chemical should allow us to ascertain which of the individual agents is driving any synergisms.

Conclusions

Our data show that combined exposure to certain environmental chemicals can induce immunotoxicity, as shown by effects on SRBC-specific IgM responses and T- or B-cell counts, compared to that by individual exposure to the chemicals in mixtures. However, this toxicity appears to differ, depending on which chemicals are combined. In particular, it was clear that, among the three combinations, MXC + PARA presented the most immunotoxic profile in the murine hosts. The combined toxicity may be affected by chemical structure, receptor binding, and immune pathways involved; further studies are currently in progress. It is expected that the results of this study will help others in their evaluation of immunotoxic combinational effects when conducting assessments of the safety of environmental/occupational chemicals.

Acknowledgements

This work was supported by a research Grant-in-Aid from the Ministry of Health, Labor, and Welfare of Japan. The authors wish to thank Mrs Y. Tajima and L. Miyashita of the Institute of Environmental Toxicology (Ibaraki, Japan) for their technical assistance.

Declaration of interest

The authors report no conflicts of interest. The authors alone are responsible for the content and writing of the paper.

References

Battaglia, C. L., Gogal Jr., R. M., Zimmerman, K., and Misra, H. P. 2010. Malathion, lindane, and piperonyl butoxide, individually or in combined mixtures, induce immune-toxicity via apoptosis in murine splenocytes *in vitro*. *Int. J. Toxicol.* 29:209–220.

Casale, G. P., Cohen, S. D., and DiCapua, R. A. 1984. Parathion-induced suppression of humoral immunity in inbred mice. *Toxicol. Lett.* 23: 239–247.

Committee on Proprietary Medicinal Products. 2000. *Note for Guidance on Repeat-Dose Toxicity*, CPMP/SWP/1042/99. Available online at: http://www.emea.eu.int.

Cunningham, A. J. 1965. A method of increased sensitivity for detecting single antibody-forming cells. *Nature* 207:1106–1107.

Diel, F., Horr, B., Borck, H., et al. 1999. Pyrethroids and piperonyl-butoxide affect human T-lymphocytes *in vitro*. *Toxicol. Lett.* 107: 65–74.

EPA (United States Environmental Protection Agency). 1998. *Health Effects Test Guidelines: Immunotoxicity.* 1998, OPPTS 870.7800. Available online at: http://www.epa.gov/opptsfrs/publications

FDA (United States Food and Drug Administration). 2002. *Guidance for Industry: Immuotoxicology Evaluation of Investigational New Drugs.* Available online at: http://www.fda.gov/cder/guidance

Feron, V. J., Groten, J. P., Jonker, D., et al. 1995. Toxicology of chemical mixtures: Challenges for today and the future. *Toxicology* 105: 415–427.

Flipo, D., Bernier, J., Girard, D., et al. 1992. Combined effects of selected insecticides on humoral immune response in mice. *Int. J. Immunopharmacol.* 14:747–752.

Fukuyama, T., Kosaka, T., Hayashi, K., et al. 2013. Immunotoxicity in mice induced by short-term exposure to methoxychlor, parathion, or piperonyl butoxide. *J. Immunotoxicol.* 10:150–159.

Fukuyama, T., Tajima, Y., Ueda, H., and Kosaka, T. 2011. Prior exposure to immunosuppressive organophosphorus or organochlorine compounds aggravates the T(H)1- and T(H)2-type allergy caused by topical sensitization to 2,4-dinitrochlorobenzene and trimellitic anhydride. *J. Immunotoxicol.* 8:170–182.

Fukuyama, T., Tajima, Y., Ueda, H., et al. 2010. Apoptosis in immunocytes induced by several types of pesticides. *J. Immunotoxicol.* 7:39–56.

Gilbert, K. M., Rowley, B., Gomez-Acevedo, H., and Blossom, S. J. 2011. Co-exposure to mercury increases immunotoxicity of trichloroethylene. *Toxicol. Sci.* 119:281–292.

Goutet, M., Pepin, E., Langonne, I., et al. 2005. Identification of contact and respiratory sensitizers using flow cytometry. *Toxicol. Appl. Pharmacol.* 205:259–270.

Groten, J. P., Feron, V. J., and Suhnel, J. 2001. Toxicology of simple and complex mixtures. *Trends. Pharmacol. Sci.* 22:316–322.

Groten, J. P., Schoen, E. D., van Bladeren, P. J., et al. 1997. Subacute toxicity of a mixture of nine chemicals in rats: Detecting interactive effects with a fractionated two-level factorial design. *Fundam. Appl. Toxicol.* 36:15–29.

Hernandez, A. F., Parron, T., Tsatsakis, A. M., et al. 2013. Toxic effects of pesticide mixtures at a molecular level: Their relevance to human health. *Toxicology* 307:136–145.

Herzyk, D. J., and Holsapple, M. 2007. Immunotoxicity evaluation by immune function tests: Focus on the T-dependent antibody response (TDAR). Overview of Workshop Session at 45th Annual Meeting of Society of Toxicology March 5-9, 2006 San Diego, CA. *J. Immunotoxicol.* 4:143–147.

Holsapple, M. P. 2003. Developmental immunotoxicity testing: A review. *Toxicology* 185:193–203.

ICH. 2006. International Conference on harmonization of technical requirements for registration of pharmaceuticals for human use. *ICH Harmonized Tripartite Guideline Immunotoxicity Studies For Human Pharmaceuticals S8.* Switzerland: ICH.

Institoris, L., Papp, A., Siroki, O., et al. 2002. Immuno- and neurotoxicological investigation of combined subacute exposure with the carbamate pesticide propoxur and cadmium in rats. *Toxicology* 178:161–173.

Institoris, L., Siroki, O., Undeger, U., et al. 1999. Immunotoxicological effects of repeated combined exposure by cypermethrin and the heavy metals lead and cadmium in rats. *Int. J. Immunopharmacol.* 21:735–743.

Janeway, C. A., Travers, P., Walport, M., and Shlomchik, M. J., (Eds.). 2004. *Immunobiology*, 6th Edition. New York: Grand Science.

Jerne, N. K., and Nordin, A. A. 1963. Plaque formation in agar by single antibody-producing cells. *Science* 140:405.

Kortenkamp, A., Faust, M., Scholze, M., and Backhaus, T. 2007. Low-level exposure to multiple chemicals: Reason for human health concerns? *Environ. Health. Perspect.* 115:106–114.

Lowry, O. H., Rosebrough, N. J., Farr, A. L., and Randall, R. J. 1951. Protein measurement with the Folin phenol reagent. *J. Biol. Chem.* 193:265–275.

Luster, M. I., Munson, A. E., Thomas, P. T., et al. 1988. Development of a testing battery to assess chemical-induced immunotoxicity: National Toxicology Program's guidelines for immunotoxicity evaluation in mice. *Fundam. Appl. Toxicol.* 10:2–19.

Mitsumori, K., Takegawa, K., Shimo, T., et al. 1996. Morphometric and immunohistochemical studies on atrophic changes in lymphohematopoietic organs of rats treated with piperonyl butoxide or subjected to dietary restriction. *Arch. Toxicol.* 70:809–814.

Nishino, R., Fukuyama, T., Tajima, Y., et al. 2013. Prior oral exposure to environmental immunosuppressive chemicals methoxychlor, parathion, or piperonyl butoxide aggravates allergic airway inflammation in NC/Nga mice. *Toxicology* 309C:1–8.

Simmons, J. E. 1995. Chemical mixtures: Challenge for toxicology and risk assessment. *Toxicology* 105:111–119.

Smialowicz, R. J., DeVito, M. J., Riddle, M. M., et al. 1997. Opposite effects of 2,2′,4,4′,5,5′-hexachlorobiphenyl and 2,3,7,8-tetrachlorodibenzo-*p*-dioxin on the antibody response to sheep erythrocytes in mice. *Fundam. Appl. Toxicol.* 37:141–149.

Takahashi, Y., Dutta, P. R., Cerasoli, D. M., and Kelsoe, G. 1998. *In situ* studies of the primary immune response to (4-hydroxy-3-nitrophenyl)-acetyl. V. Affinity maturation develops in two stages of clonal selection. *J. Exp. Med.* 187:885–895.

Takeuchi, Y., Kosaka, T., Hayashi, K., et al. 2002b. Alterations in the developing immune system of the rat after perinatal exposure to methoxychlor. *J. Toxicol. Pathol.* 17:165–170.

Takeuchi, Y., Kosaka, T., Hayashi, K., et al. 2002a. Thymic atrophy induced by methoxychlor in rat pups. *Toxicol. Lett.* 135: 199–207.

Temple, L., Kawabata, T. T., Munson, A. E., and White Jr., K. L. 1993. Comparison of ELISA and plaque-forming cell assays for measuring the humoral immune response to SRBC in rats and mice treated with benzo[a]pyrene or cyclophosphamide. *Fundam. Appl. Toxicol.* 21: 412–419.

Teuschler, L., Klaunig, J., Carney, E., et al. 2002. Support of science-based decisions concerning the evaluation of the toxicology of mixtures: A new beginning. *Regul. Toxicol. Pharmacol.* 36: 34–39.

Vieira, P., and Rajewsky, K. 1990. Persistence of memory B-cells in mice deprived of T-cell help. *Int. Immunol.* 2:487–494.

White, K. L., Musgrove, D. L., and Brown, R. D. 2010. The sheep erythrocyte T-dependent antibody response (TDAR). *Meth. Mol. Biol.* 598:173–184.

PLOS | ONE

Yoshie Takizawa, Rieko Nakata, Kiyoshi Fukuhara, Hiroshi Yamashita, Hideo Kubodera, Hiroyasu Inoue

Published: March 23, 2015 • DOI: 10.1371/journal.pone.0120865

Abstract

Long-term moderate consumption of red wine is associated with a reduced risk of developing lifestyle-related diseases such as cardiovascular disease and cancer. Therefore, resveratrol, a constituent of grapes and various other plants, has attracted substantial interest. This study focused on one molecular target of resveratrol, the peroxisome proliferator activated receptor α (PPARα). Our previous study in mice showed that resveratrol-mediated protection of the brain against stroke requires activation of PPARα; however, the molecular mechanisms involved in this process remain unknown. Here, we evaluated the chemical basis of the resveratrol-mediated activation of PPARα by performing a docking mode simulation and examining the structure-activity relationships of various polyphenols. The results of experiments using the crystal structure of the PPARα ligand-binding domain and an analysis of the activation of PPARα by a resveratrol analog 4-phenylazophenol (4-PAP) *in vivo* indicate that the 4′-hydroxyl group of resveratrol is critical for the direct activation of PPARα. Activation of PPARα by 5 μM resveratrol was enhanced by rolipram, an inhibitor of phosphodiesterase (PDE) and forskolin, an activator of adenylate cyclase. We also found that resveratrol has a higher PDE inhibitory activity (IC_{50} = 19 μM) than resveratrol analogs trans-4-hydroxystilbene and 4-PAP (IC_{50} = 27-28 μM), both of which has only 4′-hydroxyl group, indicating that this 4′-hydroxyl group of resveratrol is not sufficient for the inhibition of PDE. This result is consistent with that 10 μM resveratrol has a higher agonistic activity of PPARα than these analogs, suggesting that there is a feedforward activation loop of PPARα by resveratrol, which may be involved in the long-term effects of resveratrol *in vivo*.

Citation: Takizawa Y, Nakata R, Fukuhara K, Yamashita H, Kubodera H, Inoue H (2015) The 4′-Hydroxyl Group of Resveratrol Is Functionally Important for Direct Activation of PPARα. PLoS ONE 10(3): e0120865. doi:10.1371/journal.pone.0120865

Academic Editor: Anindita Das, Virginia Commonwealth University, UNITED STATES

Received: September 13, 2014; **Accepted:** January 27, 2015; **Published:** March 23, 2015

Data Availability: All relevant data are within the paper.

Funding: This work was supported by Grants-in-Aid for Scientific Research (Nos. 19300250 and 24300217 to H.I. and R.N.) from the Ministry of Education, Culture, Sports, Science, and Technology of Japan; the Iijima Memorial Foundations for the Promotion of Food Science and Technology; Uehara Memorial Foundation of Nutrition; and the Japan Food Chemical Research Foundation. The funders had no role in study design, data collection and analysis, decision to publish, or preparation of the manuscript.

Competing interests: All authors have declared that no competing interests exist in this revised manuscript. Two of the authors are employed by a commercial company, Medicinal Chemistry Research Laboratories, Mitsubishi Tanabe Pharma Corporation, Kanagawa, Japan. This does not alter the authors' adherence to PLOS ONE policies on sharing data and materials.

Introduction

The phytoalexin resveratrol (3, 5, 4′-trihydroxystilbene) [1] possesses antioxidant properties and has multiple effects, including the inhibition or suppression of cyclooxygenase (COX) [2], [3], and the activation of peroxisome proliferator activated receptors (PPARs) [4] and the NAD^+-dependent protein deacetylase sirtuin 1 (SIRT1) [5]. Previous studies show that resveratrol can prevent or slow the progression of various cancers, cardiovascular diseases, and ischemic injuries, as well as enhancing stress resistance and extending lifespan [6], [7].

Resveratrol is a calorie-restriction mimetic [8] with potential anti-aging and anti-diabetogenic properties; therefore, its ability to activate SIRT1 has attracted particular interest. However, the activation of SIRT1 by resveratrol *in vitro* appears to be an artifact generated by the use of fluorophore-tagged substrates [9], [10]. A recent study reported that cAMP-dependent phosphodiesterase (PDE) is a direct target of resveratrol and suggested that the metabolic effects of the compound are mediated by PDE inhibition [11]; however, this proposal remains unconfirmed. Previous studies by our group focused on the hypothesis that the beneficial effects of resveratrol require the direct activation of PPARα [4], [12], [13], which is supported by reports that PPARα mediates some of the effects of calorie restriction [14].

PPARs are members of a nuclear receptor family of ligand-dependent transcription factors [15]. The three PPAR isoforms, PPARα (NR1C1), β/δ (NR1C2), and γ (NR1C3), show distinct tissue distributions and play various roles in lipid and carbohydrate metabolism, cell proliferation and differentiation, and inflammation, and are considered molecular targets for the treatment of lifestyle-related diseases [15], [16]. The ligand-binding domains of the PPAR isoforms share 60–70% sequence identity, although all three isoforms bind naturally occurring fatty acids [17]. The prostaglandin D_2-derived metabolite, 15-deoxy-$\Delta^{12,14}$- prostaglandin

J_2, is a potent natural ligand of PPARγ [18], [19]. We previously reported that this metabolite suppresses lipopolysaccharide-induced expression of COX-2, a key inflammatory enzyme in prostaglandin synthesis, in macrophage-like U937 cells but not in vascular endothelial cells [20]. We also demonstrated that the expression of COX-2 is regulated by negative feedback mediated by PPARγ, especially in macrophages [20]. These findings indicate that PPARs participate in the cell type-specific control of COX-2 expression [3], which led us to hypothesize that resveratrol is a direct activator of PPARs. This proposal is supported by the results of *in vitro* reporter assays in bovine arterial endothelial cells (BAECs) [21], which demonstrated that 5 μM resveratrol activates PPARα, β/δ, and γ [4], [13]. In a study using PPARα-knockout mice, resveratrol treatment (20 mg/kg weight/day for 3 days) protected the brain against ischemic injury through a PPARα-dependent mechanism, indicating that resveratrol activates PPARα *in vivo* [4]. Moreover, we also demonstrated that the resveratrol tetramer, vaticanol C, activates PPARα and PPARβ/δ both *in vitro* (5 μM) and *in vivo* (0.04% of the diet for 8 weeks), although no effects on SIRT1 were observed [13].

In light of the findings described above, the aim of this study was to evaluate the chemical basis of the activation of PPARα by resveratrol.

Materials and Methods

Reagents and cell culture

Resveratrol was purchased from Sigma and the other plant polyphenols were purchased from Wako Chemicals (Japan). Azobenzene and 4-phenylazophenol (4-PAP) were purchased from Tokyo Chemicals, and trans-4-hydroxystilbene (T4HS) was synthesized as reported previously [22]. A 100 mM stock solution of each compound was prepared in DMSO and the stock was diluted to the working concentration before use. BAECs (Cell Applications, San Diego, CA) were grown in DMEM supplemented with 10% fetal calf serum.

Transcription assays and construction of mutated PPARα expression vectors

BAECs were transfected with 0.15 μg of the tk-PPREx3-Luc reporter plasmid, 0.15 μg of the human PPARα expression vector pGS-hPPARα (GeneStorm clone L02932; Invitrogen), and 0.04 μg of the pSV-βgal vector, using Trans IT-LT-1 (Mirus) as described previously [20], [23]. Twenty-eight hours after transfection, the BAECs were incubated with the relevant chemical for 24 h, after which the cells were harvested and lysed, and luciferase and β-galactosidase activities were measured. The luciferase activities were normalized to those of the β-galactosidase standard. The validity of this reporter assay was previously confirmed using Wy-14643, GW501516, and pioglitazone, which are synthetic agonists of PPARα, β/δ, and γ, respectively [23]. Site-directed mutagenesis of PPARα to form I241A, L247A, F273A, I317A and I354A was performed using an inverse PCR method, the KOD-Plus-Mutagenesis Kit (Toyobo, Japan), pGS-hPPARα as a template, and mutagenic primers. Mutagenic primers used were: F273A 5′- gctcactgctgccagtgcacgtcagtggagaccgtcac-3′(forword), 5′- gatgcggacctccgccaccaagttcaggatgccattgg-3′(reverse); I354A 5′- gccatggaacccaagtttgattttgc catgaagttcaat-3′ (forword), 5′- atcacagaacggtttccttaggctttttaggaattcacg-3′(reverse); I241A 5′- gcacatgatatggagacactgtgtatg-3′ (forword), 5′- tgcgacaaaaggtggattgttactg-3′ (reverse); L247A 5′- agcatgtatggctgagaagacgctgg-3′ (forword), 5′- gccatacatgctgtctccatatcatgtatgac-3′ (reverse); I317A 5′- gcattcgccatgctgtcttctgtg-3′ (forword), 5′- tgcggcctcataaactccgtattttagc-3′ (reverse). All mutations were confirmed by DNA sequencing.

Docking mode prediction and free energy calculations

The docking modes of resveratrol were predicted using the GOLD 3.0 docking program [24]. The protein co-ordinates were taken from the PPARα-GW409544 complex structure (PDB ID: 1K7L) and the amino acid residues within 12 Å of GW409544 were assumed to be the target binding site. The docking procedure with GOLD 3.0 was repeated 150 times, and the 150 docking poses were clustered to obtain four representative poses. Molecular dynamics simulations were performed using the AMBER 8 program and the Cornell force field 94. The solvent water was the SPC model and the cubic periodic boundary condition was used. The Coulomb interaction was evaluated using the particle mesh Ewalt method. The protein-ligand complex structure was moved with a time step of 2 femtoseconds and hydrogens were constrained with the SHAKE algorithm. After standard minimization and equilibration of the protein-ligand complex, simulation was performed for 1 nanosecond and 1,000 snapshots were collected. A Molecular Mechanical/Poisson-Boltzmann Surface Area analysis [25] was performed with a standard protocol. Computational alanine scanning was performed in a similar manner to that described above, mutating each amino acid in turn.

Animal experiments

Male 8-week-old SV/129-strain (wild-type) and PPARα-knockout mice (Jackson Laboratory) were housed in a room at 24 ± 2°C with a 12 h/12 h light/dark cycle and were fed the AIN93-G diet or the same diet supplemented with 0.04% 4-PAP. Food and water were available ad libitum. After 8 weeks of feeding, the mice were anesthetized with isoflurane, and euthanized by collecting a blood sample using a syringe. Livers were removed and stored in RNA later solution (Ambion, USA) at -30°C. Body weight, food consumption and liver weight were not significantly different between 4-PAP-fed mice and control. In addition, plasma AST and ALT level of 4-PAP-fed mice were same level as control (data not shown). This study was carried out in accordance with the guideline for Care and Use of Laboratory Animals published by Minister of the Environment Government of Japan (No. 88 of April 28, 2006). All experimental procedures were approved by the Animal Care Committee of Nara Women's University. All efforts were made to minimize suffering.

Real-time PCR

Total RNA was isolated using the acid guanidinium thiocyanate procedure. Real-time RT-PCR was performed using the Mx3005 system (Stratagene) as described previously [23]. Expression levels of each mRNA were normalized to those of GAPDH mRNA. PCR primers used were: GAPDH 5′- ggtgaaggtcggagtcaacgga-3′ (forword), 5′- gagggatctcgctcctggaaga-3′ (reverse); Acyl CoA oxidase 1 5′- gggagtgctacgggttacatg-3′ (forword), 5′- ccgatatccccaacagtgatg-3′ (reverse); Carnitine palmitoyltransferase 1A 5′- cttccatgactcggctcttc-3′ (forword), 5′- aaacagttccacctgctgct-3′ (reverse); Adiponectin receptor type 2 5′- acccacaaccttgcttcatc-3′ (forword), 5′- ggcagctccggtgatataga-3′ (reverse); Fatty acid binding protein 1 5′- aagtaccaattgcagagccagga-3′ (forword), 5′- ggtgaactcattgcggacca-3′ (reverse); Long-chain acyl CoA dehydrogenase 5′- cagttgcatgaaaccaaacg-3′ (forword), 5′- gacgatctgtcttgcgatca-3′ (reverse); SIRT1 5′- gtcagataaggaaggaaaac-3′ (forword), 5′- tggctctatgaaactgttct-3′ (reverse).

PDE inhibition assay

The PDE inhibition assay was performed using the PDE-Glo™ Phosphodiesterase assay (Promega). Bovine brain-derived PDE, majority of which was PDE4 isozyme [26], was purchased from Sigma. One milliunit of PDE was pre-incubated with varying concentrations of rolipram (Wako Chemicals, Japan), resveratrol, T4HS or 4-PAP for 30 min at room temperature, and then 1 μM cAMP substrate was added and the reactions were incubated for a further 90 minutes at 37°C. Luminescence was measured using the Tecan Infinite 200 plate-reader.

Statistical analysis

All results are expressed as the mean ± SD. Comparisons between groups were performed using unpaired *t*-tests or two-way ANOVA with post-hoc Bonferroni multiple comparison test. Values were deemed to be statistically significantly different at $p < 0.05$.

Results and Discussion

The 4′-hydroxyl group of resveratrol is required for the activation of PPARα *in vitro*

First, we investigated whether resveratrol and its related compounds (Fig. 1A) are able to activate PPARα in a cell-based luciferase reporter assay. BAECs were transiently transfected with the PPRE-luc reporter vector, the human PPARα expression vector GS-hPPARα, and pSV-β-gal as an internal control, and then incubated with 5, 10 μM resveratrol or its related compounds for 24 h. The activation of PPARα by resveratrol was suppressed by the addition of a 3′-hydroxyl group (to form piceatannol), by the replacement of the 3,5-hydroxyl groups with methoxy groups (to form pterostilbene), and by deletion of the 3,4-hydroxyl groups from resveratrol (to form T4HS) (Fig. 1A, B). The activation of PPARα by 4-PAP, which has a chemical structure similar to that of T4HS instead of the stilbene to azobenzene backbone (Fig. 1A), was similar to that by T4HS, and that, the level of activation was reduced further following deletion of the hydroxyl group (to form azobenzene) These compounds showed the dose-dependent increase of PPARα activation except for azobenzene (Fig. 1A, B).

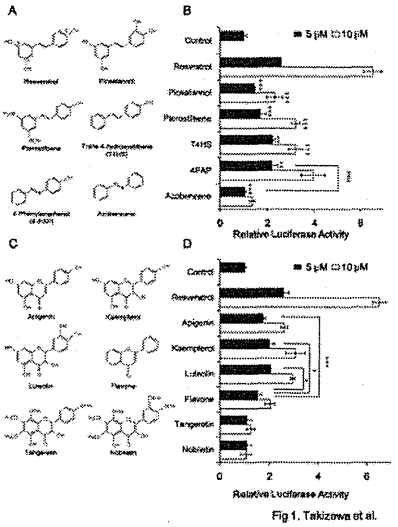

Fig 1. Takizawa et al.

Fig 1. The 4′-hydroxyl group of resveratrol is required for the activation of PPARα *in vitro*.
(A) The chemical structures of resveratrol and its related compounds containing a 4′-hydroxyl group (shown in red). (B) The activation of PPARα by exposure of BAECs transiently transfected with PPRE-luc, GS-hPPARα, and pSV-β-gal to the compounds (5, 10 μM) shown in (A). Data were statistically evaluated using the unpaired *t*-test. ** $p < 0.01$, *** $p < 0.001$ compared with cells treated with 5 μM resveratrol. ††† $p < 0.001$ compared with cells treated with 10 μM resveratrol. ### $p < 0.001$ compared with cells treated with 4-PAP. (C) The chemical structures of the flavonoids studied. (D) The activation of PPARα by exposure of BAECs transiently transfected with PPRE-luc, GS-hPPARα, and pSV-β-gal to 5 μM of resveratrol or to 5 μM of the flavonoids shown in (C). Data were statistically evaluated using the unpaired *t*-test. * $p < 0.05$, *** $p < 0.001$ compared with cells treated with flavone. (B) and (D) were presented as the relative luciferase activities normalized to those of the β-galactosidase standard, and represent the mean ± SD of three independent wells of cells. Similar results were obtained by two additional experiments.
doi:10.1371/journal.pone.0120865.g001

Next, we compared the PPARα-activating ability of other polyphenols with a flavone backbone (Fig. 1C) with that of resveratrol. The compounds studied were as follows: apigenin, which has a similar 4′-hydroxyl group to that of resveratrol; kaempferol and luteolin, both of which have chemical structures similar to that of apigenin but contain an additional one or two hydroxyl groups, respectively; a flavone with no hydroxyl group; and tangeretin and nobiletin, which have four or five methoxy groups, respectively, one of which replaces the 4′-hydroxyl group of resveratrol (Fig. 1C). The abilities of apigenin, kaempferol, and luteolin to activate PPARα were approximately 20–35% lower than that of resveratrol (Fig. 1D). The flavone that lacked hydroxyl groups displayed 55% of the activating ability of resveratrol and the ability of flavone to activate PPARα was significantly lower than that of apigenin, kaempferol and luteolin. The abilities of these compounds to activate PPARα at 10 μM were higher than 5 μM except for tangeretin and

nobiletin (chemicals with no "corresponding 4'-OH"). These results indicate that the 4'-hydroxyl group of resveratrol is functionally important for the activation of PPARα although the contribution of this 4'-hydroxyl group may differ between the stilbene and flavone backbones.

Identification of a plausible docking model and identification of F273 and I354 as PPARα residues involved in resveratrol binding

The X-ray crystal structure of the PPARα LBD as a complex with its synthetic agonist GW409544 and a co-activator motif from steroid receptor co-activator 1 was reported previously [27]. The hydrogen bonds between the carboxylate of GW409544, Tyr314 on helix 5, and Tyr464 on the AF2 helix, act as a molecular switch that activates the transcriptional activity of PPARα [27]. The docking modes of resveratrol were predicted using the GOLD 3.0 docking program [24] and protein co-ordinates from the PPARα-GW409544 complex structure (PDB ID: 1K7L). Four modes were predicted; the four orientations of the nearly planar molecule are horizontal or vertical mirror images (Fig. 2A). Of the four predicted modes, modes I and II, which are vertical mirror images, seem feasible for two reasons. First, when the calculated docking mode II of resveratrol was superimposed on the PPARα-GW409544 complex structure, the configuration of resveratrol (Fig. 2B; orange) partially overlapped that of GW409544 (Fig. 2B; green). Second, the 4'-hydroxyl group of resveratrol was in the vicinity of the hydroxyl groups of Tyr314 and Tyr464, suggesting the possibility of hydrogen bond formation between them. The 3,5-hydroxyl groups of resveratrol were located near to hydrophobic amino acid residues, suggesting that they do not contribute much to the binding affinity for PPARα. This proposal is consistent with the finding that removing these groups (to form T4HS) had a slight but significant suppressive effect on the ability of resveratrol to activate PPARα (Fig. 1B). The binding features were also consistent with the experimental observation that the 4'-hydroxyl group is a crucial functional moiety for PPARα activation (Fig. 1).

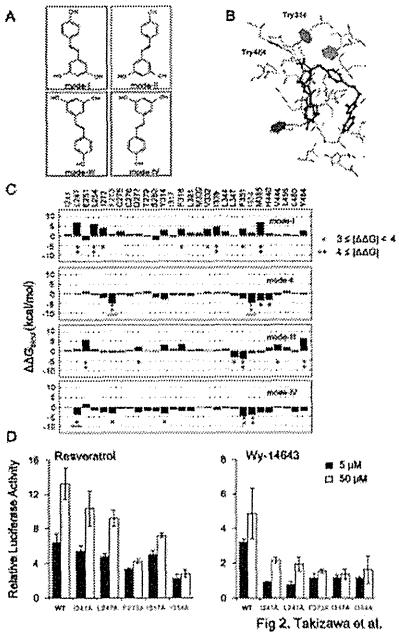

Fig 2. Docking models and analysis of PPARα residues required for binding to resveratrol.
(A) The four docking modes of resveratrol predicted using the GOLD 3.0 docking program [24] with protein co-ordination data from the PPARα-GW409544 complex structure (PDB ID: 1K7L) and a standard docking protocol. (B) Superimposition of docking mode II of resveratrol (orange) on the structure of PPARα bound to GW409544, a potent PPARα agonist (green). Only the amino acids located near to GW409544 are displayed. The hydrogen bonds of Tyr314 and Tyr464 are shown as dashed green lines. (C) Binding free energies (ΔΔGbind (kcal/mol)) of the indicated PPARα amino acid residues, calculated by alanine scanning using data for the four predicted docking modes. (D) Activation of wild-type (WT) PPARα and its mutants by 5, 50 μM resveratrol or Wy-14643. BAECs were transiently transfected with PPRE-luc, wild-type or mutant GS-hPPARα, and pSV-β-gal. The data are presented as relative luciferase activities normalized to those of the β-galactosidase standard and as 1 for cells treated with DMSO (control), and represent the mean ± SD of three independent wells of cells. Similar results were obtained by two additional experiments. The data were calculated the relative luciferase activity in cells transfected with wild-type PPARα.
doi:10.1371/journal.pone.0120865.g002

In modes III and IV, which are horizontal mirror images of modes II and I, respectively, the 4'-hydroxyl group would be located further away from Tyr314 and Tyr464; therefore, these modes may not be compatible with the apparent importance of this group to PPARα activation. However, the binding free energies predicted using a Molecular Mechanical/Poisson-Boltzmann Surface Area analysis [25] showed that modes II (-10.28 ± 9.12 kcal/mol) and IV (-15.64 ± 9.31 kcal/mol) are more plausible than mode I (-1.28 ± 11.12 kcal/mol), although it is worth noting that the free energy for GW409544 binding is-35.63 ± 11.79 kcal/mol. Ideally, these calculations should be based on crystallographically determined complex co-ordinates, although we resorted to docking predictions here. Taken together, this information suggests that mode II is the most plausible docking model for resveratrol (Fig. 2C).

A computational alanine scanning technique was then used to examine the contribution of each PPARα amino acid residue around the ligand. We were predicted that the residues F273 and I354 were the most favorable sites for binding the free energy of resveratrol in mode II whereas the residues I241, L247 and I317 were not favorable sites in mode II. Consistent with these predictions, site-directed mutagenesis of either of these residues (F273A or I354A) reduced the activation of PPARα by resveratrol compared with others (I241A, L247A, and I317A) (Fig. 2D) in BAECs transiently transfected with the PPRE-luc reporter. On the other hand, all mutants (I241A, L247A, F273A, I317A, and I354A) were suppressed by Wy-14643. These results provide additional evidence that docking mode II of resveratrol is plausible, and that its 4′-hydroxyl group is functionally important for PPARα activation. In this study, we did not show that resveratrol directly binds to PPARα, however, our collaborated study showed the direct interaction between resveratrol and PPARγ by X-ray crystal structure analysis (unpublished data), which is also recently reported by another group [28].

4-PAP induces the expression of PPARα-dependent genes and SIRT1

Next, the importance of the 4′-hydroxyl group of resveratrol to the activation of PPARα *in vivo* was examined. A previous study demonstrated that exposure of wild-type mice to 0.04% vaticanol C, a resveratrol tetramer, upregulates the hepatic expression of PPARα-responsive genes such as fatty acid binding protein 1. However, this response was not observed in PPARα-knockout mice, indicating that vaticanol C activates PPARα *in vivo* [13]. Similarly, we recently found that exposure of wild-type mice (but not PPARα-knockout mice) to 0.04% resveratrol for 4 weeks upregulates the hepatic expression of SIRT1 and PPAR-responsive genes such as Acyl CoA oxidase 1, Long-chain acyl CoA dehydrogenase, and Fatty acid binding protein 1 (unpublished data), indicating that resveratrol also activates PPARα *in vivo*. Here, a resveratrol analog 4-PAP, which has a 4′-hydroxyl group on an azobenzene backbone (Fig. 1A), was used to examine the importance of this group to the activation of PPARα *in vivo*. Compared with wild-type mice fed a control diet, those exposed to 0.04% 4-PAP for 8 weeks showed significantly higher hepatic expression levels of the PPARα-responsive genes such as Acyl CoA oxidase 1, Carnitine palmitoyltransferase 1A and Adiponectin receptor type 2 and a tendency toward higher expression levels of the genes such as Fatty acid binding protein 1 and Long-chain acyl CoA dehydrogenase (Fig. 3). These responses were not observed in PPARα knockout mice, indicating that 4-PAP activates PPARα *in vivo* (Fig. 3). Interestingly, similar to the results of our experiments using resveratrol (unpublished data), there was significantly 4-PAP-induced upregulation of SIRT1mRNA expression in wild-type, but not PPARα knockout mice (Fig. 3), indicating that PPARα-dependent upregulation of SIRT1 mRNA is attributable to SIRT1-activation by resveratrol *in vivo*.

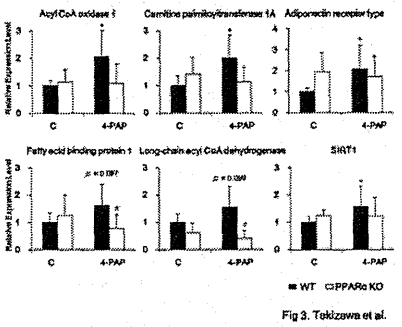

Fig 3. 4-PAP induces PPARα-dependent genes and SIRT1 *in vivo*.
RT-qPCR was used to determine the mRNA levels of the indicated genes in liver samples from wild-type (WT; filled columns) and PPARα-knockout (PPARα KO; open columns) mice fed the control AIN-93G diet (C) or the same diet supplemented with 0.04% 4-PAP for 8 weeks. Data represent the mean ± SD from 7–8 mice in each group (WT) and from 4 mice in each group (PPARα KO). Data were statistically evaluated using the unpaired two-way ANOVA with post-hoc Bonferroni multiple comparison test. *$p < 0.05$ compared with wild-type mice fed the control diet. #$p < 0.05$ compared with wild-type mice fed the 4-PAP-supplemented diet. For each mRNA, data were normalized to the expression levels in wild-type mice fed the control diet.
doi:10.1371/journal.pone.0120865.g003

Inhibition of PDE enhances the activation of PPARα by resveratrol

Finally, the inhibitory effect of PDEs on the activation of PPARα by resveratrol was examined using a luciferase reporter assay. BAECs were transiently transfected with the PPRE-luc reporter vector, the human PPARα expression vector GS-hPPARα, and pSV-β-gal as an internal control, and then incubated with varying concentrations of resveratrol, T4HS or 4-PAP for 24 h. At higher concentrations (from 10 μM to 40 μM), resveratrol had a more potent effect on the activation of PPARα than the others (Fig. 4A, left), on the other hand, resveratrol, T4HS and 4-PAP had the similar effect at lower concentrations (from 1.25 to 2.5 μM) (Fig. 4A, right). These results suggest that the 4′-hydroxyl group of resveratrol contributes to the activation of PPARα at up to 2.5 μM concentration, however, this 4′-hydroxyl group is not sufficient for the PPARα-activation at over 10 μM concentration.

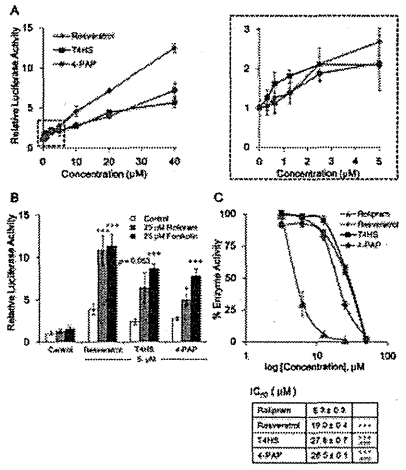

Fig 4. Takizawa et al.

Fig 4. Inhibition of PDE enhances the activation of PPARα by resveratrol, especially at higher doses.
(A) The dose-dependent activation of PPARα by resveratrol, T4HS and 4-PAP in BAECs transiently transfected with PPRE-luc, GS-hPPARα, and pSV-β-gal. Following transfection, the cells were incubated for 24 h with resveratrol, T4HS or 4-PAP at the indicated concentrations. Data were normalized to the β-galactosidase standard and represent the mean ± SD of three independent wells of cells. The right graph corresponds to the lower area marked by a dashed rectangle in left graph. (B) cAMP-dependent enhancement of PPARα activation by resveratrol, T4HS or 4-PAP. BAECs transiently transfected with PPRE-luc, GS-hPPARα, and pSV-β-gal were incubated for 24 h with 5 μM compounds in the presence or absence of 25 μM rolipram, a PDE4 inhibitor, or 25 μM forskolin, an adenylate cyclase activator. Luciferase data were normalized to the β-galactosidase standard and represent the mean ± SD of three independent wells. *$p < 0.05$, ***$p < 0.001$ (unpaired *t*-test) compared with control cells treated with the same compound. (C) The inhibition of PDE by resveratrol, T4HS, and rolipram. Data represent the mean ± SD of three independent wells of cells. Similar results were obtained by two additional experiments. The IC_{50} values are shown in the Table. ***$p < 0.001$ (unpaired *t*-test) compared with rolipram. ###$p < 0.001$ (unpaired *t*-test) compared with resveratrol. Similar results were obtained by two additional experiments in (A-C).
doi:10.1371/journal.pone.0120865.g004

A recent study reported that resveratrol inhibits PDE isozymes, PDE3 (IC_{50} = 10 μM) and PDE4 (IC_{50} = 14 μM), respectively [11]. It is therefore possible that the more potent effect of higher concentrations of resveratrol on the activation of PPARα is dependent on the inhibition of PDE, which will be contributed to the subsequent increase in intracellular cAMP levels. The activation of PPARα by 5 μM resveratrol, T4HS, or 4-PAP was enhanced by rolipram, a PDE4 inhibitor, or forskolin, an adenylate cyclase activator, both of which increase intracellular cAMP levels, although rolipram or forskolin alone could not activate PPARα (Fig. 4B). These results indicate that the activation of PPARα by resveratrol or its related compound is enhanced by cAMP. Thus, PPARα activation by resveratrol at an early point serves as a trigger to enhance the activation of PPARα in advance of the inhibition of PDE by resveratrol. Our PDE inhibition assay (Fig. 4C) revealed that resveratrol is a more potent inhibitor (IC_{50} = 19.0 μM) than T4HS (IC_{50} = 27.8 μM; $p = 0.00012$) and 4-PAP (IC_{50} = 26.5 μM; $p = 0.00022$), which explains the relatively greater effect of higher 10 μM concentration of resveratrol on the activation of PPARα (Fig. 4A). Zhao *et al.* recently reported that by different PDE4 assay using ^{3}H-cAMP, resveratrol is more potent inhibitor (IC_{50} = 14.0 μM) than pterostilbene (Fig. 1A) (IC_{50} = 27.0 μM) [29], which is similar to our PDE inhibitory data of T4HS and 4-PAP (Fig. 4C), indicating that the 4′-hydroxyl group of resveratrol partly contributes, but not sufficient, to inhibition of PDE.

This study investigated the molecular mechanisms involved in the activation of PPARα by resveratrol. An examination of the structure-activity relationships of resveratrol-related compounds revealed that the 4′-hydroxyl group of resveratrol is functionally important for the direct activation of PPARα (Fig. 1). This result was confirmed by a docking model simulation and a subsequent experiment using the crystal structure of the PPARα LBD (Fig. 2), as well as by an *in vivo* investigation of PPARα activation by resveratrol analog 4-PAP (Fig. 3). Remarkably, the induction of SIRT1 mRNA depends on the activation of PPARα by 4-PAP (Fig. 3) and resveratrol (unpublished data). Although direct activation of SIRT1 by resveratrol was unclear [9], [10], SIRT1 was reported to bind to PPARα and enhanced the transcriptional activity of PPARα with its co-activator PGC-1α and promotes fatty acid oxidation [30]. Therefore, there may be a feedforward activation of PPARα by resveratrol via activation of SIRT1.

Whereas the 4′-hydroxyl group of resveratrol directly contributes to PPARα activation, this 4′-hydroxyl group partly contributes to inhibition of PDE since the pattern of inhibition differed between resveratrol, T4HS and 4-PAP (Fig. 4). Activation of PPARα by resveratrol was enhanced by its inhibition of PDE. This feedforward activation of PPARα by resveratrol may provide a reasonable explanation why long-term intake of resveratrol at concentrations lower than those used for *in vitro* assays induces the activation of PPARα *in vivo*. Fig. 5 shows an ongoing hypothesis on long-term activation of PPARα by resveratrol *in vivo*. As a short-term effect, resveratrol activates PPARα, which induces PPARα responsive genes involved in lipid metabolism. Activation of lipid metabolism finally increases intracellular ratio of ATP/ADP, and will decrease intracellular cAMP levels, which may feedback control of PPARα–activation with a time lag. As a long-term effect, resveratrol inhibits PDE, which will enhance the PPARα-activation. At present, we do not have sufficient evidences for this hypothesis, especially feedback regulation of PPARα *in vivo*. Further study will need to evaluate this hypothesis.

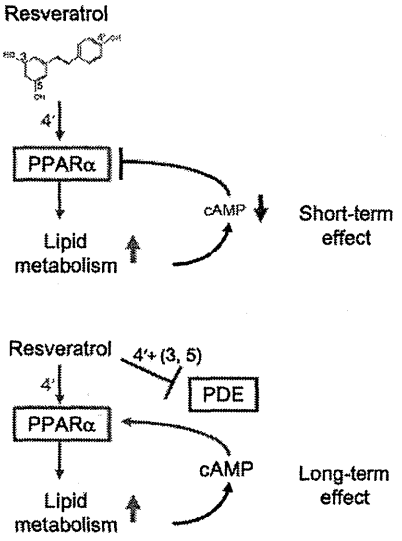

Fig 5. Takizawa et al.

Fig 5. Possible relationship among resveratrol, PPARα and PDE.
These diagrams present our hypothesis about short- and long-term effects of resveratrol, as shown in the text.
doi:10.1371/journal.pone.0120865.g005

Acknowledgments

We thank Drs. Shobu Namura and Takashi Nakazawa for helpful discussions and Ms. Haruka Takeuchi, Tomoko Tsukamoto, Naoko Anzai, Yukiko Kosuge, Emi Tamura, Ayako Takai for technical assistance.

Author Contributions

Conceived and designed the experiments: YT RN HI. Performed the experiments: YT RN HY HK HI. Analyzed the data: YT RN HY HK HI. Contributed reagents/materials/analysis tools: YT RN KF HY HK HI. Wrote the paper: YT RN HY HK HI.

References

1. Langcake P, Pryce RJ. The production of resveratrol by Vitis vinifera and other members of the Vitaceae as a response to infection or injury. Physiol Plant Pathol. 1976;9: 77–86. doi: 10.1016/0048-4059(76)90077-1
View Article • PubMed/NCBI • Google Scholar

2. Jang M, Cai L, Udeani GO, Slowing KV, Thomas CF, Beecher CW, et al. Cancer chemopreventive activity of resveratrol, a natural product derived from grapes. Science. 1997;275: 218–220. pmid:8985016 doi: 10.1126/science.275.5297.218
View Article • PubMed/NCBI • Google Scholar

3. Subbaramaiah K, Chung WJ, Michaluart P, Telang N, Tanabe T, Inoue H, et al. Resveratrol inhibits cyclooxygenase-2 transcription and activity in phorbol ester-treated human mammary epithelial cells. J Biol Chem. 1998;273: 21875–21882. pmid:9705326 doi: 10.1074/jbc.273.34.21875
View Article • PubMed/NCBI • Google Scholar

4. Inoue H, Jiang XF, Katayama T, Osada S, Umesono K, Namura S. Brain protection by resveratrol and fenofibrate against stroke requires peroxisome proliferator-activated receptor α in mice. Neurosci Lett. 2003;352: 203–206. pmid:14625020 doi: 10.1016/j.neulet.2003.09.001
View Article • PubMed/NCBI • Google Scholar

5. Howitz KT, Bitterman KJ, Cohen HY, Lamming DW, Lavu S, Wood JG, et al. Small molecule activators of sirtuins extend Saccharomyces cerevisiae lifespan. Nature. 2003;425: 191–196. pmid:12939617 doi: 10.1038/nature01960
View Article • PubMed/NCBI • Google Scholar

6. Lastra CA, Villegas I. Resveratrol as an anti-inflammatory and anti-aging agent: mechanisms and clinical implications. Mol Nutr Food Res. 2005;49: 405–430. pmid:15832402 doi: 10.1002/mnfr.200500022
View Article • PubMed/NCBI • Google Scholar

7. Baur JA, Sinclair DA. Therapeutic potential of resveratrol: the in vivo evidence. Nat Rev Drug Discov. 2006;5: 493–506. pmid:16732220 doi: 10.1038/nrd2060
View Article • PubMed/NCBI • Google Scholar

8. McCay CM, Crowell MF, Maynard LA. The effect of retarded growth upon the length of life span and upon the ultimate body size. J Nutr. 1935;10: 63–79. doi: 10.3410/f.717977201.793470731
View Article • PubMed/NCBI • Google Scholar

9. Kaeberlein M, McDonagh T, Heltweg B, Hixon J, Westman EA, Caldwell SD, et al. Substrate-specific activation of sirtuins by resveratrol. J Biol Chem. 2005;280:17038–17045. pmid:15684413 doi: 10.1074/jbc.m500655200
View Article • PubMed/NCBI • Google Scholar

10. Pacholec M, Bleasdale JE, Chrunyk B, Cunningham D, Flynn D, Garofalo RS, et al. SRT1720, SRT2183, SRT1460, and resveratrol are not direct activators of SIRT1. J Biol Chem. 2010;285: 8340–8351. doi: 10.1074/jbc.M109.088682. pmid:20061378
View Article • PubMed/NCBI • Google Scholar

11. Park SJ. Resveratrol ameliorates aging-related metabolic phenotypes by inhibiting cAMP phosphodiesterases. Cell. 2012;148: 421–433. doi: 10.1016/j.cell.2012.01.017. pmid:22304913
View Article • PubMed/NCBI • Google Scholar

12. Nakata R, Takahashi S, Inoue H. Recent advances in the study on resveratrol. Biol Pharm Bull. 2012;35: 273–270. pmid:22382311 doi: 10.1248/bpb.35.273
View Article • PubMed/NCBI • Google Scholar

13. Tsukamoto T, Nakata R, Tamura E, Kosuge Y, Kariya A, Katsukawa M, et al. Vaticanol C, a resveratrol tetramer, activates PPARα and PPARβ/δ in vitro and in vivo. Nutr Metab. 2010;7: 46. doi: 10.1186/1743-7075-7-46
View Article • PubMed/NCBI • Google Scholar

14. Corton JC, Apte U, Anderson SP, Limaye P, Yoon L, Latendresse J, et al. Mimetics of caloric restriction include agonists of lipid-activated nuclear receptors. J Biol Chem. 2004;279: 46204–46212. pmid:15302862 doi: 10.1074/jbc.m406739200
View Article • PubMed/NCBI • Google Scholar

15. Mangelsdorf DJ, Thummel C, Beato M, Herrlich P, Schütz G, Umesono K, et al. The nuclear receptor superfamily: the second decade. Cell. 1995;83: 835–839. pmid:8521507 doi: 10.1016/0092-8674(95)90199-x
View Article • PubMed/NCBI • Google Scholar

16. Michalik L, Auwerx J, Berger JP, Chatterjee VK, Glass CK, Gonzalez FJ, et al. International Union of Pharmacology. LXI. Peroxisome proliferator-activated receptors. Pharmacol Rev. 2006;58: 726–741. pmid:17132851 doi: 10.1124/pr.58.4.5
View Article • PubMed/NCBI • Google Scholar

17. Xu HE, Lambert MH, Montana VG, Parks DJ, Blanchard SG, Brown PJ, et al. Molecular recognition of fatty acids by peroxisome proliferator-activated receptors. Mol Cell. 1999;3: 397–403. pmid:10198642 doi: 10.1016/s1097-2765(00)80467-0
View Article • PubMed/NCBI • Google Scholar

18. Forman BM, Tontonoz P, Chen J, Brun RP, Spiegelman BM, Evans RM. 15-Deoxy-delta 12,14-prostaglandin J_2 is a ligand for the adipocyte determination factor PPARγ. Cell. 1995;83: 803–812. pmid:8521497 doi: 10.1016/0092-8674(95)90193-0
View Article • PubMed/NCBI • Google Scholar

19. Kliewer SA, Lenhard JM, Willson TM, Patel I, Morris DC, Lehmann JM. A prostaglandin J_2 metabolite binds peroxisome proliferator-activated receptor gamma and promotes adipocyte differentiation. Cell. 1995;83: 813–819. pmid:8521498 doi: 10.1016/0092-8674(95)90194-9
View Article • PubMed/NCBI • Google Scholar

20. Inoue H, Tanabe T, Umesono K. Feedback control of cyclooxygenase-2 expression through PPARγ. J Biol Chem. 2000;275: 28028–28032. pmid:10827178
View Article • PubMed/NCBI • Google Scholar

21. Inoue H, Taba Y, Miwa Y, Yokota C, Miyagi M, Sasaguri T. Transcriptional and Posttranscriptional Regulation of Cyclooxygenase-2 Expression by Fluid Shear Stress in Vascular Endothelial Cells. Arterioscler Thromb Vasc Biol. 2002;22: 1415–1420. pmid:12231559 doi: 10.1161/01.atv.0000028816.13582.13
View Article • PubMed/NCBI • Google Scholar

22. Thakkar K, Geahlen RL, Cushman M. Synthesis and protein-tyrosine kinase inhibitory activity of polyhydroxylated stilbene analogues of piceatannol. J Med Chem. 1993;36: 2950–2955. pmid:8411012 doi: 10.1021/jm00072a015
View Article • PubMed/NCBI • Google Scholar

23. Hotta M, Nakata R, Katsukawa M, Hori K, Takahashi S, Inoue H. Carvacrol, a component of thyme oil, activates PPARα and γ and suppresses COX-2 expression. J Lipid Res. 2010;51: 132–139. doi: 10.1194/jlr.M900255-JLR200. pmid:19578162
View Article • PubMed/NCBI • Google Scholar

24. Jones G, Willett P, Glen RC, Leach AR, Taylor R. Development and validation of a genetic algorithm for flexible docking. J Mol Biol. 1997;267: 727–748. pmid:9126849 doi: 10.1006/jmbi.1996.0897
View Article • PubMed/NCBI • Google Scholar

25. Kuhn B, Kollman PA. Binding of a diverse set of ligands to avidin and streptavidin: an accurate quantitative prediction of their relative affinities by a combination of molecular mechanics and continuum solvent models. J Med Chem. 2000;43: 3786–3791. pmid:11020294 doi: 10.1021/jm000241h
View Article • PubMed/NCBI • Google Scholar

26. Kleppisch T. Phosphodiesterases in the central nervous system. Handb Exp Pharmacol. 2009;191: 71–92. doi: 10.1007/978-3-540-68964-5_5. pmid:19089326

View Article • PubMed/NCBI • Google Scholar

27. Xu HE, Lambert MH, Montana VG, Plunket KD, Moore LB, Collins JL, et al. Structural determinants of ligand binding selectivity between the peroxisome proliferator activated receptors. Proc Natl Acad Sci USA. 2001;98: 13919–13924. pmid:11698662 doi: 10.1073/pnas.241410198
View Article • PubMed/NCBI • Google Scholar

28. Calleri E, Pochetti G, Dossou KS, Laghezza A, Montanari R, Capelli D, et al. Resveratrol and its metabolites bind to PPARs. ChemBioChem. 2014;15: 1154–1160. doi: 10.1002/cbic.201300754. pmid:24796862
View Article • PubMed/NCBI • Google Scholar

29. Zhao P, Chen SK, Cai YH, Lu X, Li Z, Cheng YK, et al. The molecular basis for the inhibition of phosphodiesterase-4D by three natural resveratrol analogs. Isolation, molecular docking, molecular dynamics simulations, binding free energy, and bioassay. Biochim Biophys Acta. 2013;1834: 2089–2096. doi: 10.1016/j.bbapap.2013.07.004. pmid:23871879
View Article • PubMed/NCBI • Google Scholar

30. Purushotham A, Schug TT, Xu Q, Surapureddi S, Guo X, Li X. Hepatocyte-specific deletion of SIRT1 alters fatty acid metabolism and results in hepatic steatosis and inflammation. Cell Metab. 2009;9: 327–338. doi: 10.1016/j.cmet.2009.02.006. pmid:19356714
View Article • PubMed/NCBI • Google Scholar